Earthquake clusters analysis in Central and East Java region, Indonesia, based on hypocenter determination and relocation with waveform cross-correlation

Faiz Muttaqy[1], Andri Dian Nugraha[2], Nanang T. Puspito[2], David P. Sahara[2], Zulfakriza Zulfakriza[2], Supriyanto Rohadi[3], Pepen Supendi[4]

[1]Graduate Program of Geophysical Engineering, Faculty of Mining and Petroleum Engineering, Institut Teknologi Bandung, Jalan Ganesha No. 10, Bandung 40132, Indonesia

E-mail: *faiz.muttaqy@yahoo.com*

[2]Global Geophysics Research Group, Faculty of Mining and Petroleum Engineering, Institut Teknologi Bandung, Jalan Ganesha No. 10, Bandung 40132, Indonesia

[3]Agency for Meteorology, Climatology and Geophysics (BMKG), Jakarta, Indonesia

[4]Agency for Meteorology, Climatology and Geophysics (BMKG), Bandung, Indonesia

Abstract The Central and East Java region, which is part of Sunda Arc, has relatively high seismicity rates due to the convergence between two major tectonic plates in Indonesia region, the Indo-Australian plate that subducts under the Eurasian plate. Many devastating earthquakes in the study area occurred as results of these plates interaction, such as the 1994 Banyuwangi earthquake (Mw 7.6) and the 2006 Yogyakarta earthquake (Mw 6.3). This study aims to determine the precise earthquake

location and analyze the pattern of seismicity distribution around Central and East Java, Indonesia. We manually re-picked P and S-wave arrival time recorded by Agency for Meteorology, Climatology and Geophysics (BMKG) of Indonesia network for the times period of January 2009-September 2017. We then determined the earthquake location by a non-linear method. To improve the accuracy of earthquakes location, we relocated 1,127 out of 1,529 events using a double-difference algorithm with waveform cross-correlation data. Overall, the seismicity around Central and East Java regions are dominantly distributed in the south of the island, e.g. Kebumen, Yogyakarta, Pacitan, Malang, and Banyuwangi cluster. These clusters are probably related to the subduction activity. Meanwhile, the shallow depth earthquakes that are clustered in mainland indicate the activity of inland faults in the region, e.g. Opak Fault, Kendeng Thrust, and Rembang-Madura-Kangean-Sakala (RMKS) fault zone. Several other active inland faults have not shown significant seismicity over the times period, i.e., Pasuruan Fault, Lasem Fault, Muria Fault, Semarang Thrust, Probolinggo Fault, etc.

Keywords: Hypocenter determination, 1D seismic velocity model, waveform cross-correlation, relocation, Central Java, East Java

1 Introduction

Central and East Java are part of Sunda Arc which has relatively high seismicity and the complex geological system as a result of Indo-Australian plate that subducts under the Eurasian plate. The convergence rate varies from ~5.6 cm/yr in the western part of Java to ~6.5 cm/yr in the East (Koulali et al. 2017). It produces several active faults, i.e., Semarang Thrust Fault, Kendeng Thrust Fault, Opak Fault, Lasem Fault, Probolinggo

Fault, Pasuruan Fault, and volcanoes that probably control the seismicity around the study area (Marliyani 2016; Pusat Studi Gempa Nasional (PuSGeN) 2017) (Fig.1). In contrast with the oblique convergence that occurs in Sumatra, the western part of the Sunda Arc, the convergence is normal to the plate boundary at Java (Malod et al. 1995). Consequently, the seismicity rate in the Central and East Java is lower than in Sumatra and West Java (the transitional zone from oblique to normal subduction) (Newcomb and Mccann 1987). However, the study area still holds the potential for destructive earthquakes. Based on the historical earthquake data, many large earthquakes occurred in Central and East Java, such as the 1994 large subduction thrust earthquake (Mw 7.6) that produced a tsunami in Banyuwangi. It was caused by slip over a subducting seamount, which is a locked patch within a decoupled subduction zone (Abercrombie et al. 2001); the 2006 Yogyakarta earthquake (Mw 6.3) that occurred on the inland Opak Fault, the geometry of which has been subsequently determined by SAR interferometry (Tsuji et al. 2009); and more historical earthquakes in the 1900s (M>6) that had been documented by Newcomb and McCann (1987) along the Sunda Arc.

Previous studies have evaluated the seismicity around study area using the regional network of BMKG (Agency for Meteorology, Climatology, and Geophysics of Indonesia) including hypocenter determination using a non-linear method in West Java (Rosalia et al. 2017), Central and East Java (Muttaqy et al. 2019), hypocenter relocation using a double-difference method in West Java (Supendi et al. 2018) and East Java (Cahyaningrum et al. 2015) and teleseismic double-difference along Sunda Arc(Nugraha et al. 2018). Many local seismic networks have also been deployed and contributed to the seismicity and tomography studies in Central and East Java, such as DOMERAPI network that had been conducted to comprehensively study the crustal

structure beneath Merapi volcano (Ramdhan et al. 2015, 2016, 2017a, b, 2019); MERAMEX network that was consisting onshore and offshore seismographic stations in Central Java had been successfully determined crustal and upper mantle structure beneath Central and East Java, also related to the volcanic activities around the study area (Koulakov et al. 2007; Wagner et al. 2007; Koulakov 2009; Rohadi et al. 2013; Bohm et al. 2013; Zulfakriza et al. 2014; Haberland et al. 2014; Wölbern and Rümpker 2016; and ambient noise tomography by using both BMKG network and portable seismographs in East Java (Martha et al. 2017).

The Central and East Java are considered to be the most densely populated region in Indonesia, with over 73 million people live in this high seismicity area (Central Bureau of Statistics of Indonesia (BPS) 2012). Due to its potential high seismic hazard, the investigation of earthquake clusters is essential to improve and support Indonesia seismic hazard map. This study aims to determine the precise hypocenter location and analyze the pattern of seismicity distribution around Central and East Java.

2 Data and Method

In this study, we used waveform data from 34 broadband seismometers of BMKG network that distributed in the Central, East Java and its surroundings within the time period of January 2009 to September 2017 (Fig 1). We carefully manually re-picked P and S-wave arrival times using Seisgram2K (Lomax and Michelini 2009). The criteria for selected events for the hypocenter determination were (i) at least recorded by four stations which have clear onset P and S arrivals, and (ii) has magnitude (Mw) > 3 (Fig 2a). For the quality control of the picking process, we plotted a Wadati diagram to

97 determine the Vp/Vs ratio of the observed data (Fig 2b). To determine the hypocenter
98 location, we applied a non-linear method using the NLLoc program (Lomax et al. 2000)
99 and the global 1D seismic velocity model of AK135 (Kennett et al. 1995). The
100 algorithm used in this program is the oct-tree importance sampling to produce an
101 estimation of the posterior density function (PDF) for the hypocenter location in 3D
102 (Lomax and Curtis 2001). The same method was also previously implemented to
103 determine hypocenter in West Java (Rosalia et al. 2017), aftershock analysis of the 27
104 May 2006, M 6.4 Yogyakarta earthquake (Husni et al. 2018; Wulandari et al. 2018),
105 Pannonian basin of Hungary (Wéber and Süle 2014), central-eastern Alps of North Italy
106 (Viganò et al. 2015), eastern border faults of the Main Ethiopian Rift (Lapins et al.
107 2020), and more.
108
109 To have a more reliable seismic velocity model beneath the study area, we updated the
110 1D seismic velocity model from VELEST code that simultaneously inverts the
111 hypocenter, velocity and station correction. The code performs an iterative damped
112 least-squares inversion, where each iteration solves ray tracing and inverse problem. We
113 can apply the damping to control which parameter of earthquake locations, layer
114 velocities, and station corrections to be adjusted. The higher the damping value, the less
115 the parameters are allowed to vary in the inversion process (Kissling 1995). In this
116 study, we selected the events that have a maximum azimuthal gap of 180^{o} to assure the
117 events are well localized by the seismograph network and expected to represent the
118 subsurface information around the study area. The 1D priori seismic velocity model that
119 considered in this study was from Koulakov et al. (2007) that successfully defined
120 crustal and upper mantle P-average velocity (Vp) beneath the Central Java, and combine
121 with AK135 model (Kennett et al. 1995) for the deeper part of the earth (> 210 km) and

S-velocity (Vs) distribution. Then, the updated model was applied in the further relocation stages.

We run HypoDD program (Waldhauser 2001), which implement the double-difference algorithm (Waldhauser and Ellsworth 2000), to relocate earthquakes previously determined by the non-linear method. The double-difference algorithm is based on the assumptions that if the distance between the two earthquakes is much smaller than their distances to the station and the length scale of the structure, then the raypaths of these earthquakes are similar. HypoDD can minimize the residuals between observed and calculated travel-time differences for pairs of earthquakes recorded at the same station. Thus, the errors due to the inaccurate velocity model can be minimized without using station correction.

We also obtained more reliable relative travel time data by applying waveform cross-correlation data into the double-difference algorithm. The use of waveform cross-correlation data is to minimize the error associated with the arrival time picking process (Hauksson and Shearer 2005; Schaff and Waldhauser 2005). The process relies on the similarity between waveforms which ware recorded at the same station. This technique had been widely used to relocate the hypocenter in the double-difference algorithm, for example in Sumatra (Pesicek et al. 2010; Waldhauser et al. 2012; Muksin et al. 2014)(Pesicek et al. 2010; Waldhauser et al. 2012; Muksin et al. 2014), Central Java (Sipayung et al. 2018), Nicoya Peninsula of Costa Rica (Hansen et al. 2006), the 2019 Ridgecrest earthquake sequence of eastern California (Lin 2020), Alboran slab of westernmost Mediterranean (Sun and Bezada 2020) and more.

3 Results and Discussions

Hypocenter determination result consists of 1,529 events located using 11,192 phases for each P and S-wave (Fig 3). The observed arrival times were plotted in the Wadati diagram to independently check the linear relationship between phases data (Fig 2b). Based on the Wadati diagram, the Vp/Vs ratio is 1.75. To quantify the capability of BMKG network on detecting the earthquakes, we have plotted the cumulative number of earthquakes over the time period of 2009-2017 and the chart of frequency-magnitude relationship using maximum likelihood method which applied in the Zmap package (Wiemer 2001). The regional BMKG network has a magnitude of completeness (Mc) of 3.4 with much more earthquakes that can be recorded, compared to the global network such as USGS which has Mc of 4.2 and fewer earthquakes that can be recorded (Fig 4). We also estimated the uncertainty of observed data by using the waveform cross-correlation technique. The average of picking errors for P and S-waves are 0.1886 s and 0.297 s, respectively. It shows that the quality of P and S-times were capable of being continued the further processing stages.

We conducted the updated 1D seismic velocity model by employing selected 154 located events that have a maximum azimuthal gap of 180^{o} and were expected to represent the average velocity of Central and East Java. It is a trial and error process by defining various initial model and parameter, iteratively. We used 1D seismic velocity model from Koulakov et al. (2007) and AK135 (Kennett et al. 1995) as the reference model, we then randomly generated ten initial models by ± 20% relative to the reference model. For each initial model, we used various velocity damping from 0.01 to 0.1, while the hypocenter and station correction damping was set to 0.01. Thus, it resulted in 100

1D seismic velocity model solutions for each Vp and Vs. We selected 1 of 100 updated model that considered to be the best solution with the minimal residual (Fig 5).

Several earthquakes that may be generated by the same source mechanism will produce high waveform similarity at a common station. Therefore, the waveform cross-correlation process ensures the consistency of P and S-waves phase identification. We computed the cross-correlation functions for P and S waves using a time window of 0.2 sec before and 2 sec after onset of P-arrival time and 1.4 sec before and 5 sec after S-arrival time onset. We used Butterworth filter between 1-6 Hz and coefficient correlation criteria that are greater than 0.7. Figure 6 shows an example of the cross-correlation result at RTBI and PWJI station. The output of the waveform cross-correlation process that saved as inputs for HypoDD is lag time and coefficient correlation.

We applied both catalog and cross-correlation differential time data into HypoDD to improve the quality of event clustering and minimalize the eliminated events to relocate. The weighting of the distance between paired events for catalog data (WDCT) was set to 45 km in the first four iterations, then it set to 15 km and 35 km for correlation data (WDCC) in the second 4 iterations. The selection of the optimum damping factor depends on the system condition to be solved, which is represented as the condition number (CND) (Hauksson and Shearer 2005). We used the damping factor of 85 and 70, resulting in a condition number that is between 40 and 80.

Finally, we successfully relocated 1,127 out of 1,529 events around Central and East Java region (table A1 in the additional file). Compare with the initial locations, the

196 relocated events are more clustered in several areas (Fig 7). The average shifted
197 earthquakes locations in X, Y, and Z direction are 3.37, 4.76, and 10.4 km, respectively
198 with the maximum shifted locations are 29.2, 44.36, and 49.98 km, respectively (Fig
199 A1). The sort of significant improvement is also statistically proved by the histogram of
200 residual times (Fig 8). The relocation result has more events with residual times are
201 close to zero, rather than before relocation. Moreover, the distribution of location error
202 in X, Y and Z direction are provided in figure A2.
203
204 Based on the relocation result, the seismicity in Central and East Java are dominantly
205 distributed in the south of the island. The vertical cross-section of block B-F (Fig 9)
206 shows subduction-related events that have compatibility with slab 1.0 model (Hayes et
207 al. 2012). The dipping angle of the slab is getting steepens from west to east. Each block
208 represents several interesting clusters in the study area, such as Kebumen, Yogyakarta,
209 Pacitan, Malang, and Banyuwangi (Fig 9b).
210
211 In block B, there is Kebumen Cluster where the Kebumen earthquake (Mw 6.2)
212 occurred on 25 January 2014 (Fig 9). According to the focal mechanism we obtained
213 from Global Centroid Moment Tensor (GCMT) (Dziewonski et al. 1981; Ekström et al.
214 2012) (https://www.globalcmt.org/), it shows a normal faulting mechanism, while the
215 surrounding events in the cluster are dominated by thrusting mechanism (Fig 12). Based
216 on the location and depth, the seismicity in this cluster are intraslab events associated
217 with intense deformation zone due to plates collision (Serhalawan et al. 2017).
218
219 In block C, D, and E, the vertical cross-section depicts the cluster of Yogyakarta,
220 Pacitan, and Malang, respectively (Fig 9). These seismicity clusters are in the forearc of

the Java subduction system. The steeper dipping angle of the slab is likely to cause the earthquake occurrence rate to be higher towards the east. Reported GCMT focal mechanism shows dominantly thrusting mechanism, even though some of them also have normal faulting mechanism (Fig 12).

Block F represents an interesting cluster in the south of Banyuwangi, where the large Banyuwangi earthquake occurred in 1994 (Fig 9). The seismicity in this area probably related to the subducting plate behind seamount and triggered the normal faulting earthquake at the outer rise of the Indo-Australian plate (Abercrombie et al. 2001). It also proved by the focal mechanism solution from GCMT that shows that Banyuwangi cluster is dominantly controlled by normal fault mechanism (Fig 12).

In addition, the shallow clustered earthquakes are probably controlled by the active inland faults, such as in the block A, northern block D and block F, that associated with Opak Fault, Kendeng Thrust Fault, and Rembang-Madura-Kangean-Sakala (RMKS) Fault zone, respectively (Fig 9). Opak Fault is considered to be the cause of the 2006 Yogyakarta earthquake (Mw 6.3). Its geometry is still debatable, whether the fault plane is east or west-dipping. Based on the vertical cross-section A, the relocated events are clustered in the east of Opak Fault lineament. It shows that the fault plane is more likely east-dipping. Based on the SAR interferometry observation, it concluded that Opak Fault geometry is considered as an east-dipping left-lateral fault that ensures the hypocenter distribution in the eastern part of the fault (Tsuji et al. 2009). Several previous studies also supported this result which aftershock distribution of Yogyakarta earthquake in 2006 is parallel to Opak Fault lineament and located 5-10 km to the east (Husni et al. 2018; Wulandari et al. 2018).

Meanwhile, the Kendeng Thrust Fault is a major fault zone in the study area. This fault extends 200 km long from Central to East Java and is an accumulation of thrusts and folds (Pusat Studi Gempa Nasional (PuSGeN) 2017). Evidence of this fault movement could be observed with the presence of uplifted alluvial terrace along with the activity of this fault (Marliyani 2016). Based on the geodetic study, Koulali et al. (2017) estimated the average slip rate of Kendeng Thrust Fault at about 2.3-4.1 mm/yr. Furthermore, in the northern block D, the shallow clustered event that may support the activity of the Kendeng Thrust Zone is represented (Fig 9 and 10). This interpretation is still debatable whether the seismicity is controlled by the local fault or volcanic activity of Mt. Pandan and Mt. Wilis. While in 2015, there is Madiun earthquake (Mw 4.2) that destroyed several houses due to its shallow depth and the amplification effect in the north of Mt Pandan (Nugraha et al. 2016). Previous studies suggested that this event may be related to the local strike-slip fault (Nugraha et al. 2016; Sipayung et al. 2018). In contrast, the conducted gravity survey around Mt. Pandan indicated low-density anomaly that may be related to hot material or magma body and triggered the seismicity (Santoso et al. 2018). They suggested that the subduction process resulted in fault movement and triggered the magma flow to the surface at the same time. Thus, we concluded that the seismicity in this cluster might be associated with both Kendeng Thrust activity and magmatic process.

In the northern part of East Java, there are clustered shallow seismicity around Rembang and Madura (Fig 11). They probably associated with the same mechanism of Rembang-Madura-Kangean-Sakala fault zone, even though the lineament of this fault seems to end in Madura. However, we suggested that this fault has its continuity to the further

west where the shallow events were determined. Recently, there are some destructive earthquakes occurred around RMKS fault zone, such as Madura earthquake (Mw 4.3) and Situbondo earthquake (Mw 6.3) in 2018. The different mechanism probably triggers these earthquakes. Meanwhile, the Madura earthquake (Mw 4.3) is more likely related to the strike-slip RMKS fault, the Situbondo earthquake (Mw 6.3) has a thrusting mechanism based on the GCMT focal mechanism solution (Fig 12). It suggests that the Situbondo earthquake has a strong connection with Back Arc Thrust that may be extended from the east.

Several other active inland faults may control the seismicity around Central and East Java region, for example, the Pasuruan Fault, Lasem Fault, Muria Fault, Semarang Thrust Fault, Probolinggo Fault, etc. They have not shown a significant number of earthquakes during the time period of 2009-2017. Hence, "unpaired" events that are not clustered beyond distance weighting would be eliminated by the double-difference algorithm. Moreover, the earthquakes associated with the volcanic activities were also not well-determined due to the limited seismograph network we used in this study. They can only be detected by the local seismographs around the volcano.

4 Conclusions

We have been successfully determined 1,529 earthquakes around Central and East Java region in the times period of January 2009-September 2017 by manual re-picking process. We then relocated 1,127 events by applying waveform cross-correlation data in the double-difference algorithm. Overall, our result shows the seismicity pattern around Central and East Java is dominantly distributed in the south of the island, such as

Kebumen, Yogyakarta, Pacitan, Malang, and Banyuwangi cluster. These seismic clusters are subduction-related events that have compatibility with slab 1.0 model (Hayes et al. 2012). The dipping angle of the slab is getting steepens to the east.

Moreover, the shallow clustered earthquakes in the mainland of Central and East Java regions are probably controlled by the active inland faults including Opak Fault, Kendeng Thrust Fault, and Rembang-Madura-Kangean-Sakala (RMKS) Fault zone. Based on the relocation result, the seismicity around Opak Fault indicates east-dipping geometry, since the relocated events are distributed in the east of Opak Fault lineament. Meanwhile, the seismicity around Kendeng Thrust Fault around the north of Madiun are coincide with the volcanoes. We suggested that it triggered by both active local fault and magmatic process beneath Mt. Pandan and Mt. Wilis. Several other active inland faults have not shown significant seismicity, and the earthquakes due to the volcanic activities were not well-determined by the seismic network used in this study.

Authors' contributions

FM, ADN, NTP, SR, PS conceived the study; FM, ADN, DPS, ZZ contributed to the writing of the manuscript. All authors contributed to the preparation of the manuscript. All authors read and approved the final manuscript.

Acknowledgements

We are grateful to the Agency for Meteorology, Climatology, and Geophysics (BMKG) Indonesia, as the provider of waveform and catalog data. All figures in this study were

made by using The Generic Mapping Tools developed by Paul Wessel and Walter H.F. Smith.

Competing interests

We declare that we have no significant competing financial, professional or personal interests that might have influenced the performance or presentation of the work described in this manuscript.

Availability of data and materials

The datasets supporting the conclusions of this article are included within the article and its additional files.

Funding

This study was supported by PMDSU 2017 scholarship from the Ministry of Research, Technology, and Higher Education of the Republic of Indonesia awarded to FM and was also partially supported by PUPT 2017 from the Ministry of Research, Technology, and Higher Education of the Republic of Indonesia awarded to ADN.

References

Abercrombie RE, Antolik M, Felzer K, Ekstrom G (2001) The 1994 Java tsunami earthquake : Slip over a subducting seamount. Journal of Geophysical Research 106:6595–6607. https://doi.org/10.1029/2000JB900403

Bohm M, Haberland C, Asch G (2013) Imaging fluid-related subduction processes beneath Central Java (Indonesia) using seismic attenuation tomography. Tectonophysics 590:175–188. https://doi.org/10.1016/J.TECTO.2013.01.021

343 Cahyaningrum AP, Nugraha AD, Puspito NT (2015) Earthquake hypocenter relocation
344 using double difference method in East Java and surrounding areas. AIP
345 Conference Proceedings 1658:. https://doi.org/10.1063/1.4915029

346 Central Bureau of Statistics of Indonesia (BPS) (2012) Penduduk Indonesia menurut
347 Provinsi 1971, 1980, 1995, 2000 dan 2010

348 Dziewonski AM, Chou TA, Woodhouse JH (1981) Determination of earthquake source
349 parameters from waveform data for studies of global and regional seismicity.
350 Journal of Geophysical Research 86:2825–2852.
351 https://doi.org/10.1029/JB086iB04p02825

352 Ekström G, Nettles M, Dziewoński AM (2012) The global CMT project 2004-2010:
353 Centroid-moment tensors for 13,017 earthquakes. Physics of the Earth and
354 Planetary Interiors 200–201:1–9. https://doi.org/10.1016/j.pepi.2012.04.002

355 Haberland C, Bohm M, Asch G (2014) Accretionary nature of the crust of Central and
356 East Java (Indonesia) revealed by local earthquake travel-time tomography.
357 Journal of Asian Earth Sciences 96:287–295.
358 https://doi.org/10.1016/J.JSEAES.2014.09.019

359 Hansen SE, Schwartz SY, DeShon HR, González V (2006) Earthquake relocation and
360 focal mechanism determination using waveform cross correlation, Nicoya
361 Peninsula, Costa Rica. Bulletin of the Seismological Society of America
362 96:1003–1011. https://doi.org/10.1785/0120050129

363 Hauksson E, Shearer P (2005) Southern California hypocenter relocation with
364 waveform cross-correlation, part 1: Results using the double-difference
365 method. Bulletin of the Seismological Society of America 95:896–903.
366 https://doi.org/10.1785/0120040167

367 Hayes GP, Wald DJ, Johnson RL (2012) Slab1.0: A three-dimensional model of global
368 subduction zone geometries. Journal of Geophysical Research: Solid Earth
369 117:1–15. https://doi.org/10.1029/2011JB008524

370 Husni YM, Nugraha AD, Rosalia S, et al (2018) Aftershock location determination of
371 the 27 May 2006, M 6.4 Yogyakarta earthquake using a non-linear algorithm:
372 A preliminary results. AIP Conference 020049:020049–020049.
373 https://doi.org/10.1063/1.5047334

374 Kennett BLN, Engdahl ER, Buland R (1995) Constraints on seismic velocities in the
375 Earth from travel times. Geophysical Journal International 122:108–124.
376 https://doi.org/10.1111/j.1365-246X.1995.tb03540.x

377 Koulakov I (2009) Short Note Out-of-Network Events Can Be of Great Importance for
378 Improving Results of Local Earthquake Tomography. Bulletin of the
379 Geological Society of America 99:2556–2563.
380 https://doi.org/10.1785/0120080365

Koulakov I, Bohm M, Asch G, et al (2007) P and S velocity structure of the crust and the upper mantle beneath central Java from local tomography inversion. Journal of Geophysical Research: Solid Earth 112:1–19. https://doi.org/10.1029/2006JB004712

Koulali A, McClusky S, Susilo S, et al (2017) The kinematics of crustal deformation in Java from GPS observations: Implications for fault slip partitioning. Earth and Planetary Science Letters 458:69–79. https://doi.org/10.1016/j.epsl.2016.10.039

Lapins S, Kendall JM, Ayele A, et al (2020) Lower-Crustal Seismicity on the Eastern Border Faults of the Main Ethiopian Rift. Journal of Geophysical Research: Solid Earth 125:0–2. https://doi.org/10.1029/2020jb020030

Lin G (2020) Waveform cross-correlation relocation and focal mechanisms for the 2019 ridgecrest earthquake sequence. Seismological Research Letters 91:2055–2061. https://doi.org/10.1785/0220190277

Lomax A, Curtis A (2001) Fast probabilistic earthquake location in 3D models using Oct-Tree importance sampling. Geophys. Res. Abstr. 3

Lomax A, Michelini A (2009) M wpd : a duration – amplitude procedure for rapid determination of earthquake magnitude and tsunamigenic potential from P waveforms. Geophysical Journal International 176:200–214. https://doi.org/10.1111/j.1365-246X.2008.03974.x

Lomax A, Virieux J, Volant P, Berge-Thierry C (2000) Probabilistic Earthquake Location in 3D and Layered Models BT - Advances in Seismic Event Location. In: Thurber CH, Rabinowitz N (eds) Advances in Seismic Event Location. Modern Approches in Geophysics. Springer Netherlands, Dordrecht, pp 101–134

Malod JA, Karta K, Beslier MO, Zen MT (1995) From normal to oblique subduction: Tectonic relationships between Java and Sumatra. Journal of Southeast Asian Earth Sciences 12:85–93. https://doi.org/10.1016/0743-9547(95)00023-2

Marliyani GI (2016) Neotectonics of Java, Indonesia: Crustal Deformation in the Overriding Plate of an Orthogonal Subduction System

Martha AA, Cummins P, Saygin E, Widiyantoro S (2017) Imaging of upper crustal structure beneath East Java – Bali , Indonesia with ambient noise tomography. Geoscience Letters. https://doi.org/10.1186/s40562-017-0080-9

Muksin U, Haberland C, Nukman M, et al (2014) Journal of Asian Earth Sciences Detailed fault structure of the Tarutung Pull-Apart Basin in Sumatra , Indonesia , derived from local earthquake data. Journal of Asian Earth Sciences 96:123–131. https://doi.org/10.1016/j.jseaes.2014.09.009

418 Muttaqy F, Nugraha AD, Puspito NT, Supendi P (2019) A Non-Linear Method for
419 Hypocenter Determination around Central and East Java Region : Preliminary
420 Result. IOP Conference Series: Earth and Environmental Science 318:012008–
421 012008. https://doi.org/10.1088/1755-1315/318/1/012008

422 Newcomb KR, Mccann WR (1987) Seismic History and Seismotectonics of The Sunda
423 Arc. Journal of Geophysical Research 92:421–439.
424 https://doi.org/10.1029/JB092iB01p00421

425 Nugraha AD, Shiddiqi HA, Widiyantoro S, et al (2018) Hypocenter Relocation along
426 the Sunda Arc in Indonesia , Using a 3D Seismic-Velocity Model.
427 Seismological Research Letters 89:603–612.
428 https://doi.org/10.1785/0220170107

429 Nugraha AD, Supendi P, Shiddiqi HA, Widiyantoro S (2016) Unexpected earthquake of
430 June 25th, 2015 in Madiun, East Java. AIP Conference Proceedings 1730:.
431 https://doi.org/10.1063/1.4947369

432 Pesicek JD, Thurber CH, Zhang H, et al (2010) Teleseismic double - difference
433 relocation of earthquakes along the Sumatra - Andaman subduction zone using
434 a 3 - D model. Journal of G 115:1–20. https://doi.org/10.1029/2010JB007443

435 Pusat Studi Gempa Nasional (PuSGeN) (2017) Peta Sumber dan Bahaya Gempa
436 Indonesia Tahun 2017, First. Pusat Penelitian dan Pengembangan Perumahan
437 dan Pemukiman Badan Penelitian dan Pengembangan Kementerian Pekerjaan
438 Umum dan Perumahan Rakyat, Bandung

439 Ramdhan M, Nugraha AD, Widiyantoro S, et al (2016) Observation of Seismicity
440 Based on DOMERAPI and BMKG Seismic Networks : A Preliminary Result
441 from DOMERAPI Project. AIP Conference Proceedings 1730:1–8.
442 https://doi.org/10.1063/1.4947377

443 Ramdhan M, Nugraha AD, Widiyantoro S, Valencia AA (2015) Earthquake Location
444 Determination Using Data from DOMERAPI and BMKG Seismic Networks :
445 A Preliminary Result of DOMERAPI Project. AIP Conference Proceedings
446 1658:1–5. https://doi.org/10.1063/1.4915015

447 Ramdhan M, Widiyantoro S, Nugraha AD, et al (2019) Detailed seismic imaging of
448 Merapi volcano, Indonesia, from local earthquake travel-time tomography.
449 Journal of Asian Earth Sciences 177:134–145.
450 https://doi.org/10.1016/j.jseaes.2019.03.018

451 Ramdhan M, Widiyantoro S, Nugraha AD, et al (2017a) Seismic Travel-time
452 Tomography beneath Merapi Volcano and its Surroundings : A Preliminary
453 Result from DOMERAPI Project. IOP Conference Series: Earth and
454 Environmental Science 62:. https://doi.org/10.1088/1755-1315/62/1/012039

455 Ramdhan M, Widiyantoro S, Nugraha AD, et al (2017b) Relocation of hypocenters
456 from DOMERAPI and BMKG networks : a preliminary result from
457 DOMERAPI project. Earthquake Science 30:67–79.
458 https://doi.org/10.1007/s11589-017-0178-3

459 Rohadi S, Widiyantoro S, Nugraha a D, Masturyono (2013) Tomographic Imaging of
460 P- and S-wave Velocity Structure Beneath Central Java , Indonesia : Joint
461 Inversion of the MERAMEX and MCGA Earthquake Data. International
462 Journal of Tomography and Simulation 24:16–16

463 Rosalia S, Widiyantoro S, Dian Nugraha A, et al (2017) Hypocenter Determination
464 Using a Non-Linear Method for Events in West Java, Indonesia: A Preliminary
465 Result. IOP Conference Series: Earth and Environmental Science 62:.
466 https://doi.org/10.1088/1755-1315/62/1/012052

467 Santoso D, Wahyudi EJ, Alawiyah S, et al (2018) Gravity Structure around Mt . Pandan
468 , Madiun , East Java , Indonesia and Its Relationship to 2016 Seismic Activity.
469 Open Geosciences 10:882–888. https://doi.org/10.1515/geo-2018-0069

470 Schaff DP, Waldhauser F (2005) Waveform cross-correlation-based differential travel-
471 time measurements at the northern California seismic network. Bulletin of the
472 Seismological Society of America 95:2446–2461.
473 https://doi.org/10.1785/0120040221

474 Serhalawan YR, Sianipar D, Suardi I (2017) The January 25 th , 2014 Kebumen
475 Earthquake : A Normal Faulting in Subduction Zone of Southern Java. AIP
476 Conference Proceedings 030002: https://doi.org/10.1063/1.4987061

477 Sipayung R, Alhafiz MR, Agus R, Sianipar D (2018) Relocation of the February 2016
478 Mt. Pandan earthquake sequence using double difference with waveform cross
479 correlation. AIP Conference Proceedings 020036:020036–020036.
480 https://doi.org/10.1063/1.5047321

481 Sun M, Bezada M (2020) Seismogenic Necking During Slab Detachment: Evidence
482 From Relocation of Intermediate-Depth Seismicity in the Alboran Slab.
483 Journal of Geophysical Research: Solid Earth 125:.
484 https://doi.org/10.1029/2019JB017896

485 Supendi P, Nugraha AD, Puspito NT, et al (2018) Identification of active faults in West
486 Java , Indonesia , based on earthquake hypocenter determination , relocation ,
487 and focal mechanism analysis. Geoscience Letters.
488 https://doi.org/10.1186/s40562-018-0130-y

489 Tsuji T, Yamamoto K, Matsuoka T, et al (2009) Earthquake fault of the 26 May 2006
490 Yogyakarta earthquake observed by SAR interferometry. Earth, Planets and
491 Space 61:e29--e32. https://doi.org/10.1186/BF03353189

492 Viganò A, Scafidi D, Ranalli G, et al (2015) Earthquake relocations, crustal rheology,
493 and active deformation in the central–eastern Alps (N Italy). Tectonophysics
494 661:81–98. https://doi.org/10.1016/J.TECTO.2015.08.017

495 Wagner D, Koulakov I, Rabbel W, et al (2007) Joint inversion of active and passive
496 seismic data in Central Java. Geophysical Journal International 170:923–932.
497 https://doi.org/10.1111/j.1365-246X.2007.03435.x

498 Waldhauser F (2001) HypoDD - A Program to Compute Double-Difference Hypocenter
499 Locations by

500 Waldhauser F, Schaff DP, Diehl T, Engdahl ER (2012) Splay faults imaged by fluid-
501 driven aftershocks of the 2004 M w 9 . 2 Sumatra-Andaman earthquake.
502 Geology 40:243–246. https://doi.org/10.1130/G32420.1

503 Wéber Z, Süle B (2014) Source properties of the 29 January 2011 ML 4.5 Oroszlány
504 (Hungary) mainshock and its aftershocks. Bulletin of the Seismological
505 Society of America 104:113–127. https://doi.org/10.1785/0120130152

506 Wiemer S (2001) A software package to analyze seismicity: ZMAP. Seismological
507 Research Letters 72:373–382. https://doi.org/10.1785/gssrl.72.3.373

508 Wölbern I, Rümpker G (2016) Crustal thickness beneath Central and East Java
509 (Indonesia) inferred from P receiver functions. Journal of Asian Earth Sciences
510 115:69–79. https://doi.org/10.1016/J.JSEAES.2015.09.001

511 Wulandari A, Anggraini A, Suryanto W (2018) Hypocenter Analysis of Aftershocks
512 Data of the Mw 6.3, 27 May 2006 Yogyakarta Earthquake Using Oct-Tree
513 Importance Sampling Method. Applied Mechanics and Materials 881:89–97.
514 https://doi.org/10.4028/www.scientific.net/AMM.881.89

515 Zulfakriza Z, Saygin E, Cummins PR, et al (2014) Upper crustal structure of central
516 Java , Indonesia , from transdimensional seismic ambient noise tomography.
517 Geophysical Journal International 197:630–635.
518 https://doi.org/10.1093/gji/ggu016

519

Figure:

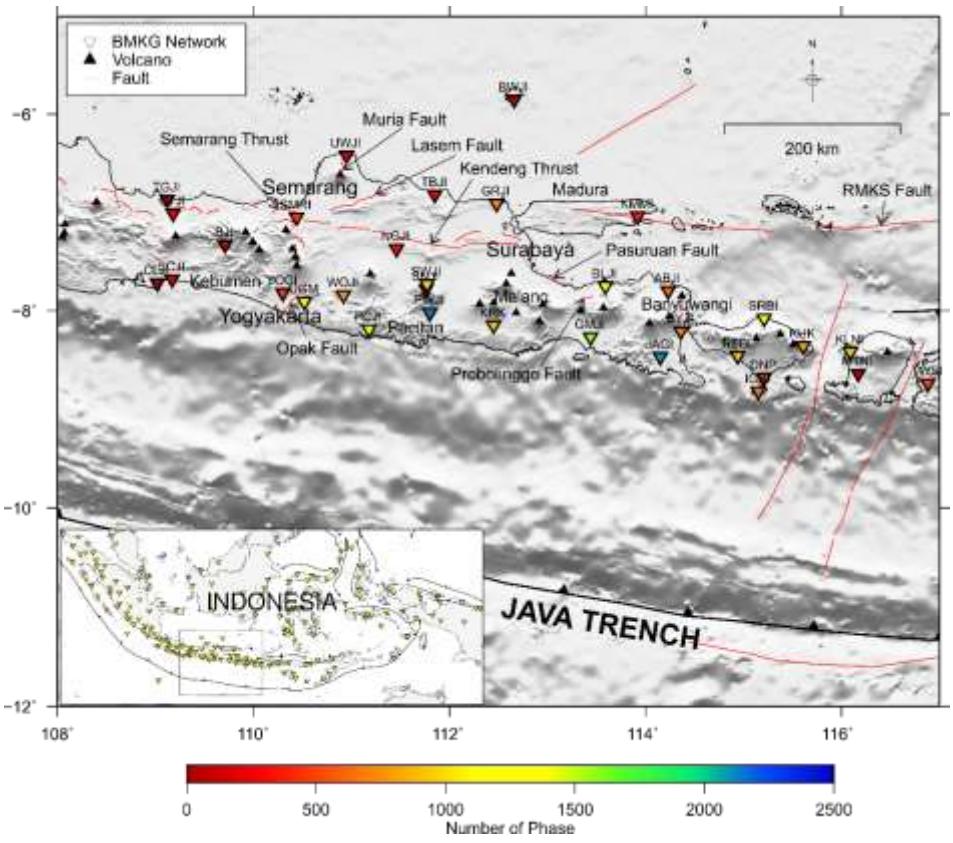

Fig. 1. Map showing the distribution of BMKG seismographic stations (inverted triangles) used in this study, active fault lineament (red lines) and volcanoes (black triangles) (Pusat Studi Gempa Nasional (PuSGeN) 2017). The colours represent the number of phases picked for each station.

526

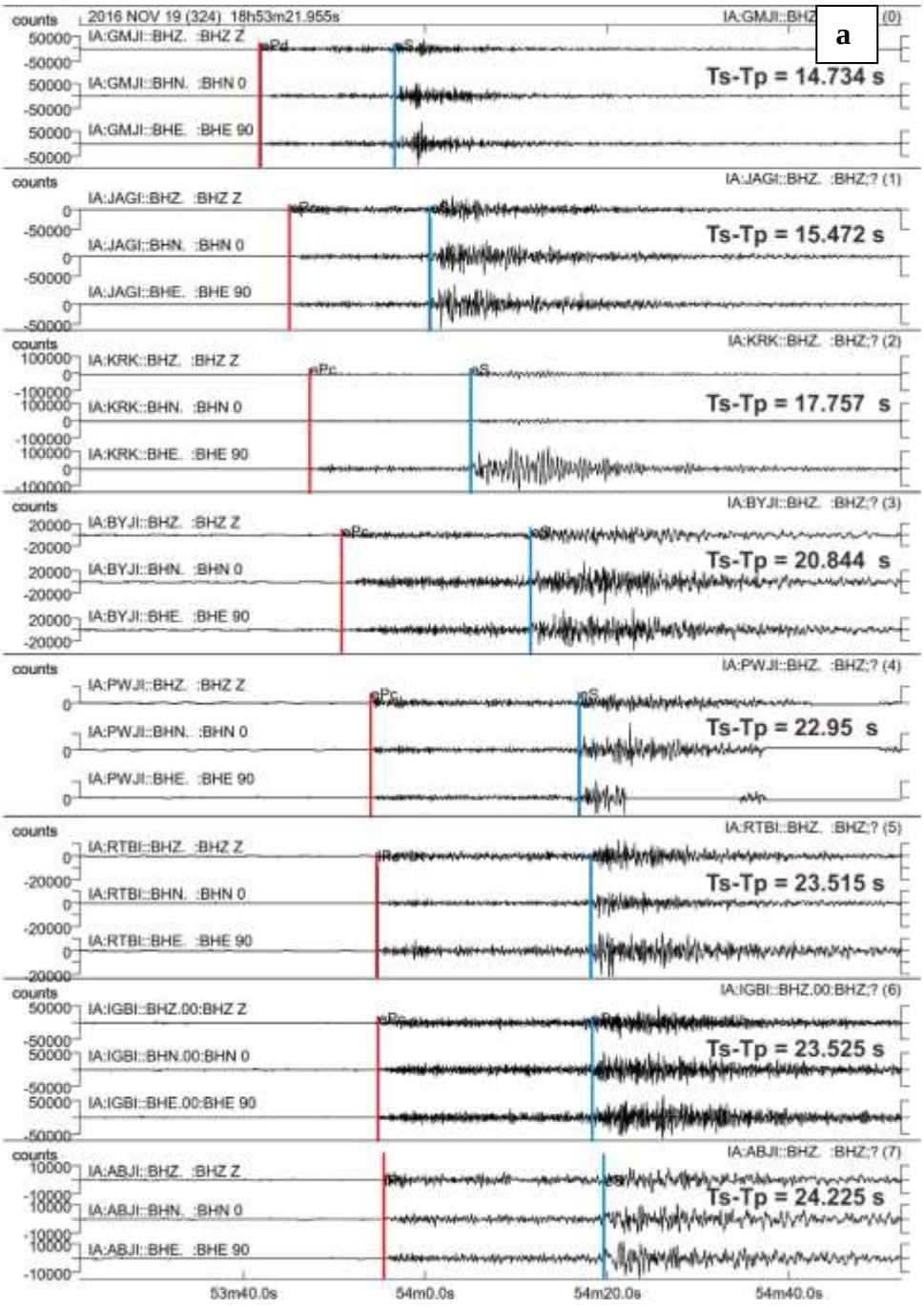
a
2016 NOV 19 (324) 18h53m21.955s
IA:GMJI::BHZ (0)
IA:GMJI::BHZ. :BHZ Z
IA:GMJI::BHN. :BHN 0
IA:GMJI::BHE. :BHE 90
Ts-Tp = 14.734 s
IA:JAGI::BHZ. :BHZ;? (1)
IA:JAGI::BHZ. :BHZ Z
IA:JAGI::BHN. :BHN 0
IA:JAGI::BHE. :BHE 90
Ts-Tp = 15.472 s
IA:KRK::BHZ. :BHZ;? (2)
IA:KRK::BHZ. :BHZ Z
IA:KRK::BHN. :BHN 0
IA:KRK::BHE. :BHE 90
Ts-Tp = 17.757 s
IA:BYJI::BHZ. :BHZ;? (3)
IA:BYJI::BHZ. :BHZ Z
IA:BYJI::BHN. :BHN 0
IA:BYJI::BHE. :BHE 90
Ts-Tp = 20.844 s
IA:PWJI::BHZ. :BHZ;? (4)
IA:PWJI::BHZ. :BHZ Z
IA:PWJI::BHN. :BHN 0
IA:PWJI::BHE. :BHE 90
Ts-Tp = 22.95 s
IA:RTBI::BHZ. :BHZ;? (5)
IA:RTBI::BHZ. :BHZ Z
IA:RTBI::BHN. :BHN 0
IA:RTBI::BHE. :BHE 90
Ts-Tp = 23.515 s
IA:IGBI::BHZ.00:BHZ;? (6)
IA:IGBI::BHZ.00:BHZ Z
IA:IGBI::BHN.00:BHN 0
IA:IGBI::BHE.00:BHE 90
Ts-Tp = 23.525 s
IA:ABJI::BHZ. :BHZ;? (7)
IA:ABJI::BHZ. :BHZ Z
IA:ABJI::BHN. :BHN 0
IA:ABJI::BHE. :BHE 90
Ts-Tp = 24.225 s
counts
53m40.0s
54m0.0s
54m20.0s
54m40.0s

527

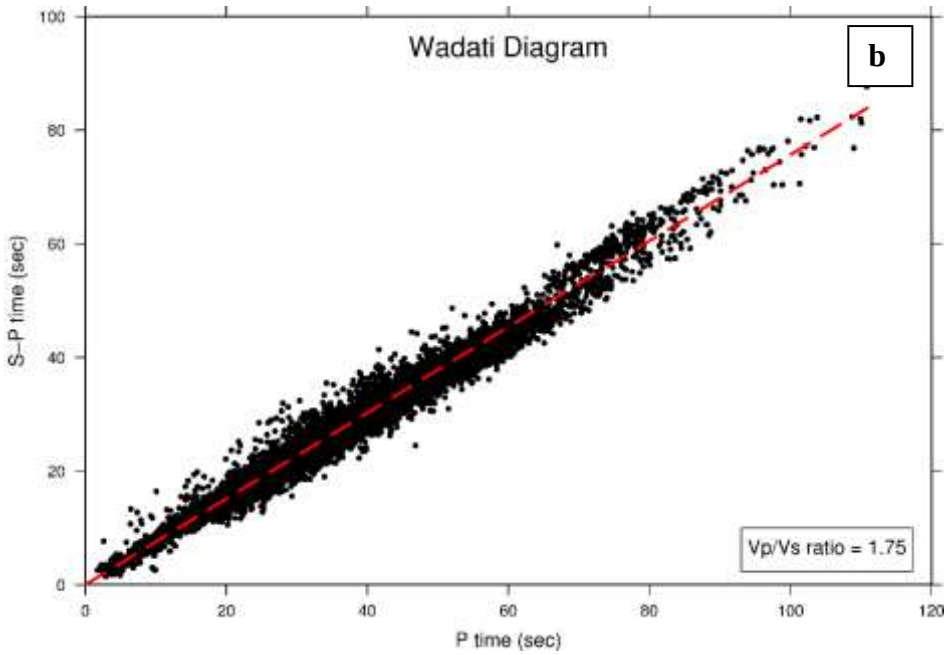

Fig. 2. **a** Three-component seismogram examples of 19 November 2016 event (the epicentre location is shown in Fig 3) recorded by the nearest stations (GMJI, JAGI, KRK, BYJI, PWJI, RTBI, IGBI, and ABJI are shown in Fig 1). Red and blue lines indicate the arrival times of P and S-wave, respectively. **b** Wadati diagram showing a linear relationship between picked phases. In this study, the Vp/Vs ratio is 1.75. Red dashed line indicates deviations from a constant Vp/Vs ratio and/or reading data errors.

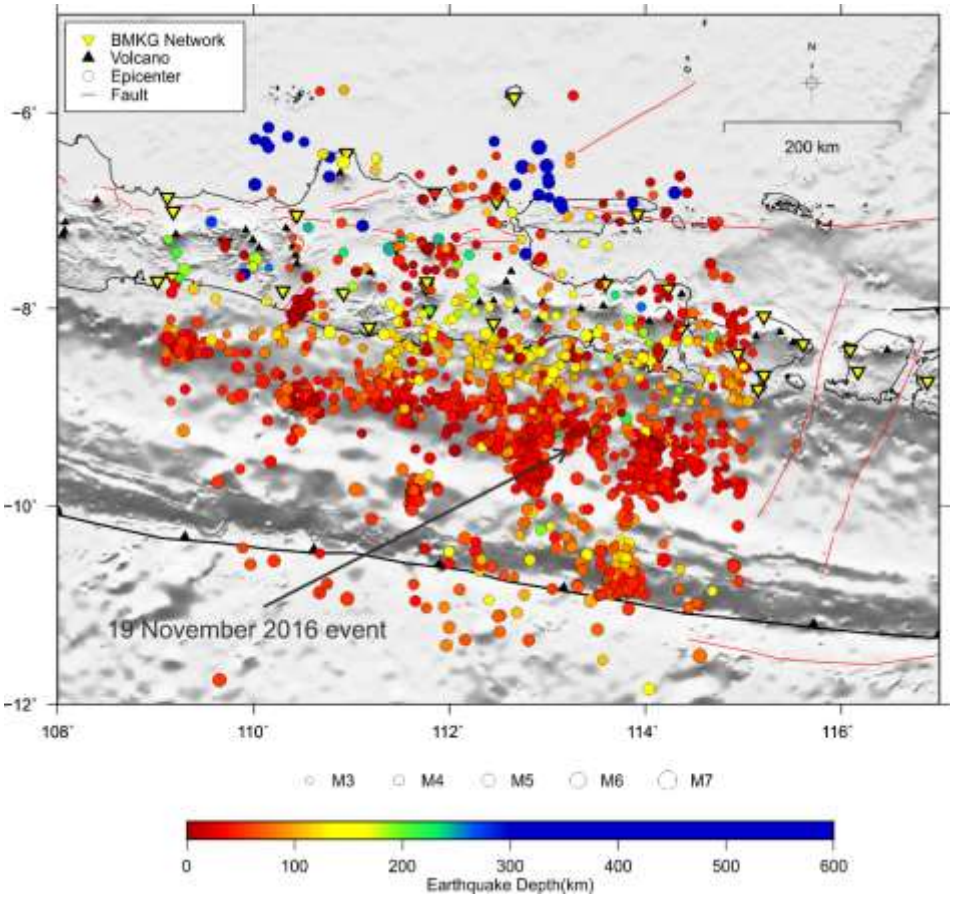

535

536 Fig. 3. Map of seismicity distribution determined by this study around Central and East
537 Java region in the times period of 2009-2017. The circles filled colours represent
538 earthquake focus depth.

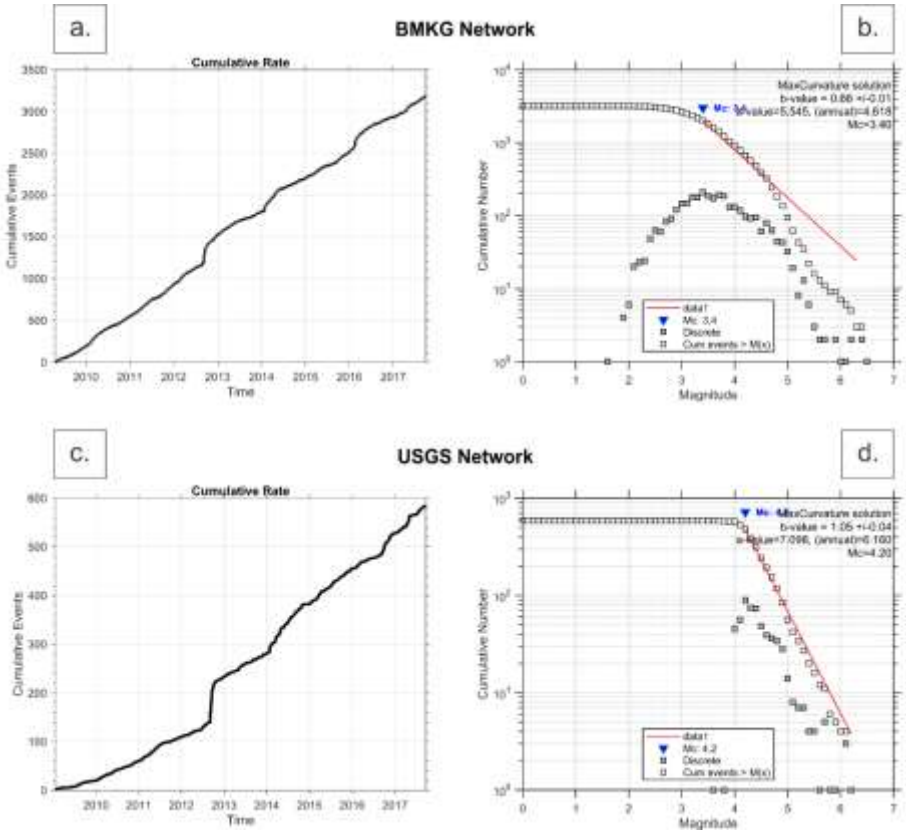

Fig. 4. **a** Earthquake cumulative number and **b** earthquake magnitude-frequency relation of regional BMKG network, compared to **c** earthquake cumulative number and **d** earthquake magnitude-frequency relation of global USGS network.

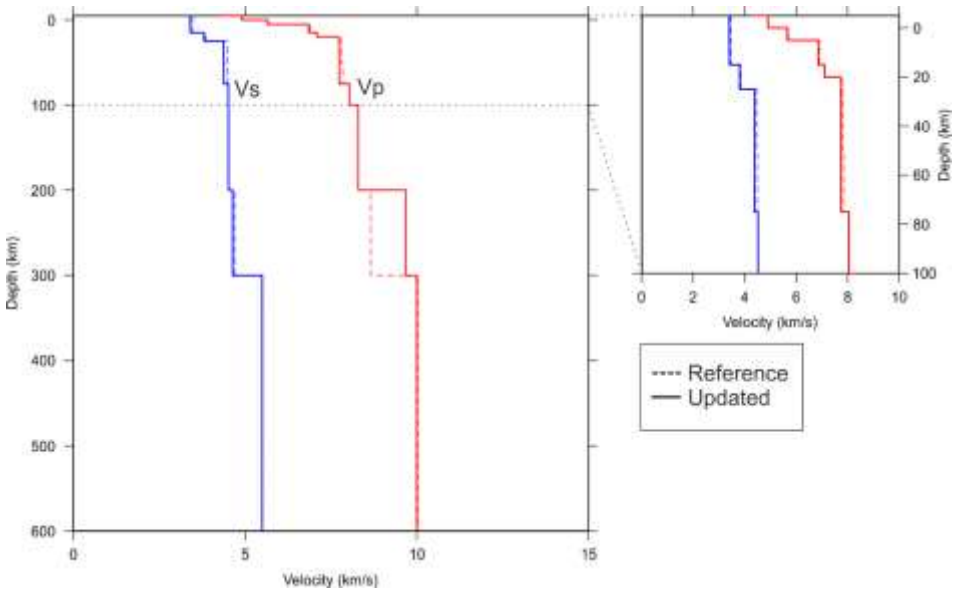

Fig. 5. The updated 1D seismic velocity model applied to the hypocenter relocation process (bold lines). The red and blue lines indicate Vp and Vs, respectively. The dashed lines are reference 1D seismic velocity model taken from Koulakov et al. (2007) and AK135 (Kennett et al. 1995).

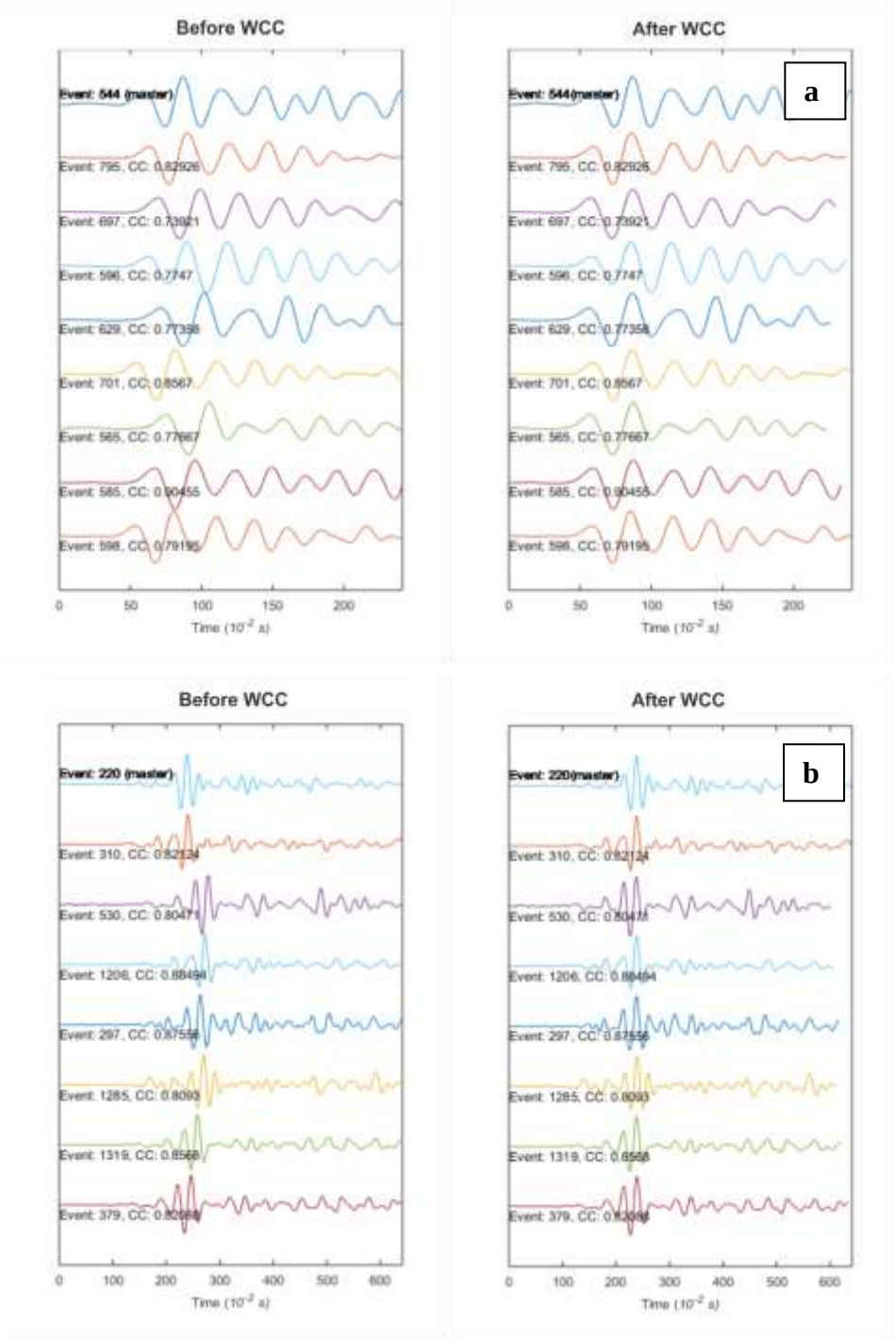

549

550 Fig. 6. Example of waveform cross-correlation (WCC) process for events recorded at
551 the common station. **a** P-wave recorded at RTBI station. **b** S-wave recorded at PWJI
552 station.

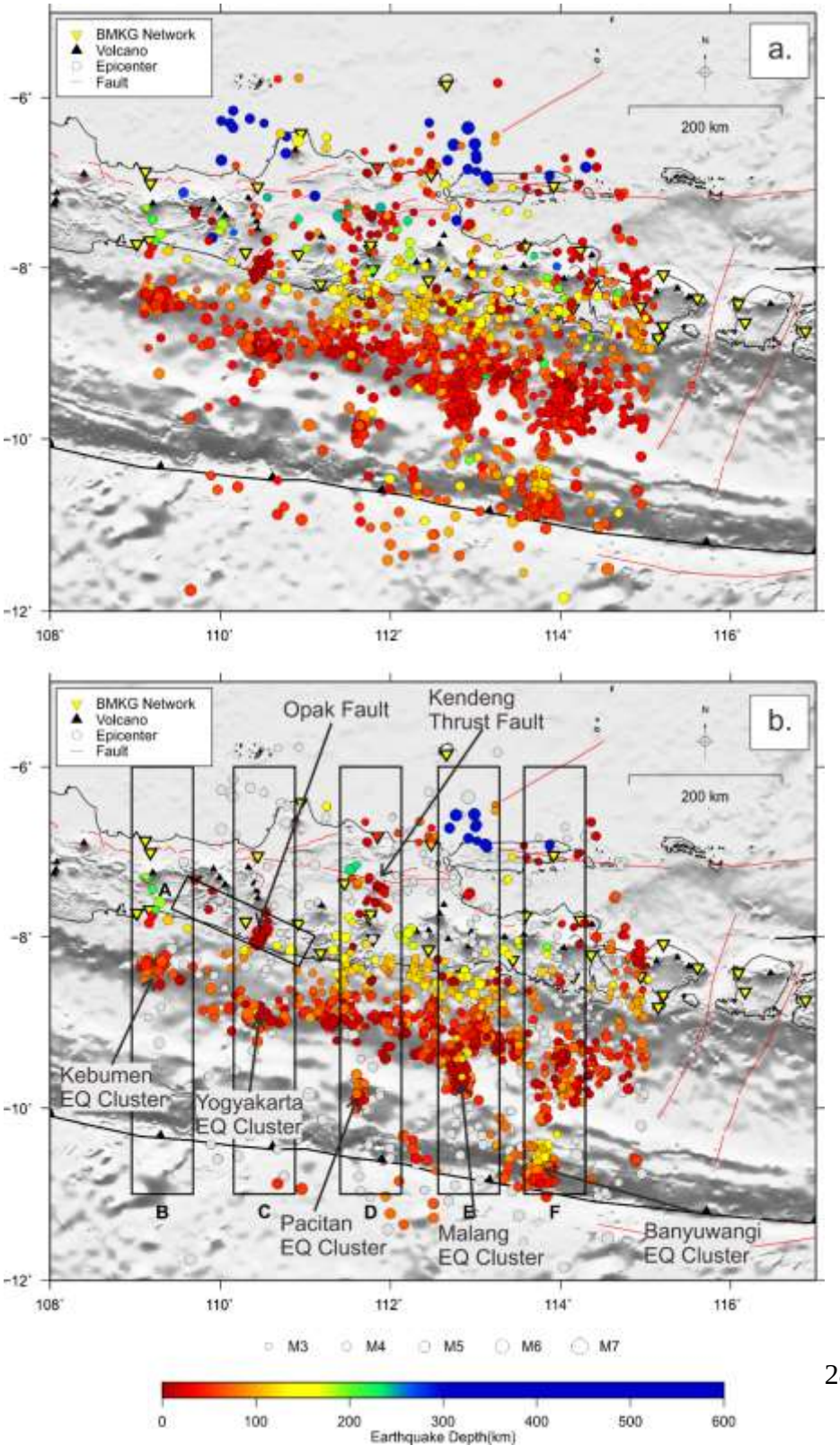

Fig. 7. Comparison of seismicity distribution around Central and East Java region. **a** before relocation. **b** after the relocation. The blocks A-F are the area used to plot the vertical cross-sections shown in Fig 9. The circles filled colours represent earthquake focus depth, while the grey circles are the earthquakes which eliminated in the relocation.

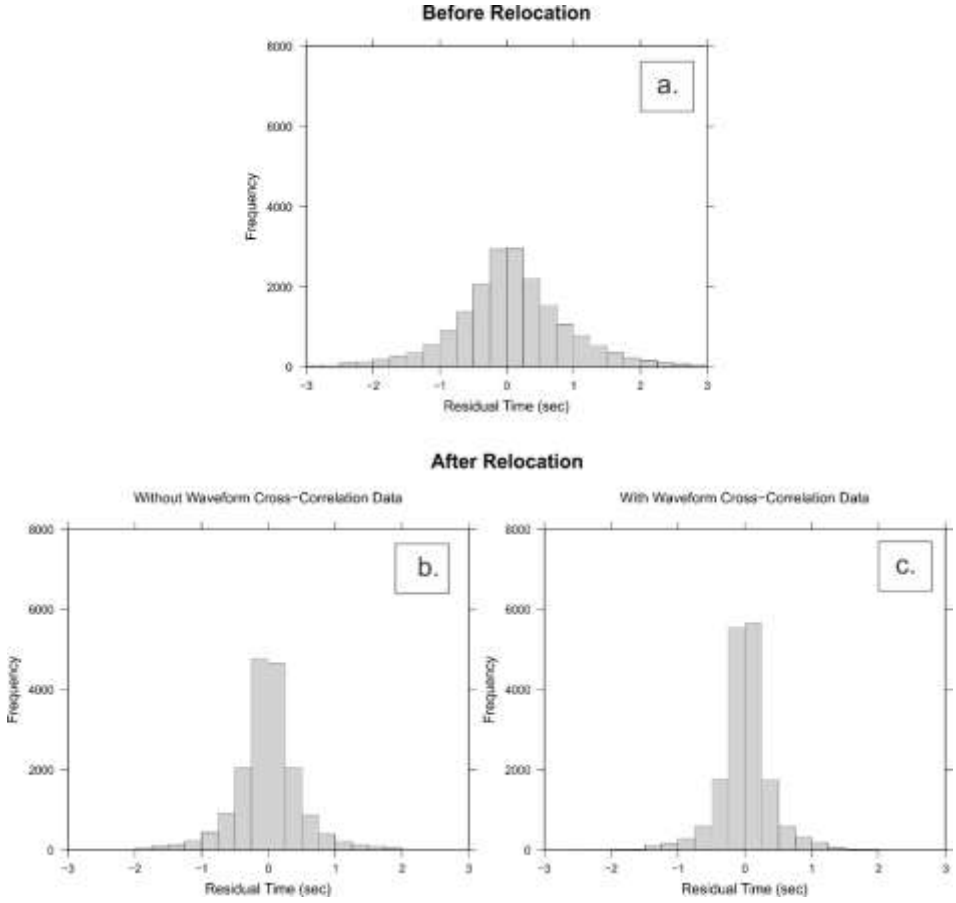

Fig. 8. **a** Histograms of travel time residuals before relocation and **b** after relocation without and **c** with waveform cross-correlation data in the relocation process for 1,127 events.

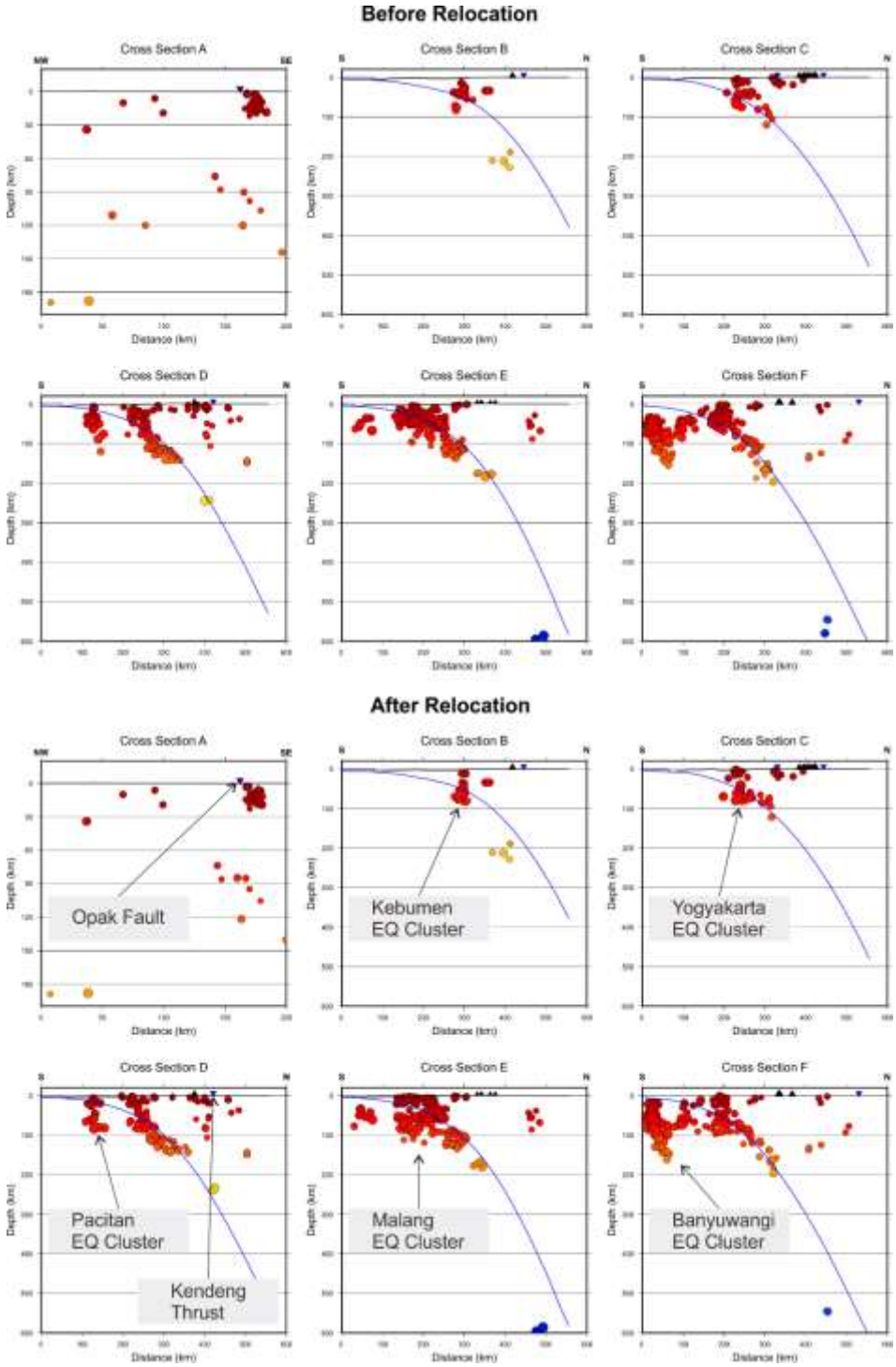

564

565 Fig. 9. Vertical cross-sections of block A-F before and after relocation (as shown in
566 Figure 6) along Opak Fault, Kebumen, Yogyakarta, Pacitan and Kendeng Thrust Fault,
567 Malang, and Banyuwangi cluster. The blue line indicates the slab 1.0 model (Hayes et
568 al. 2012).

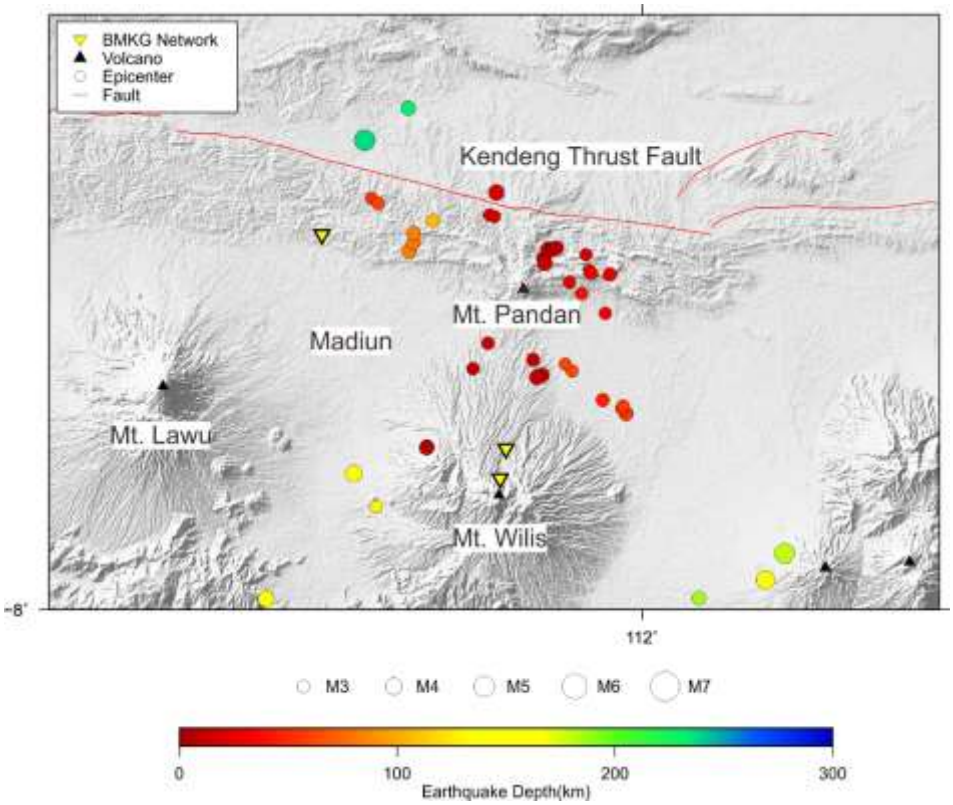

569
570
571 Fig. 10. Map of seismicity distribution around Mt. Pandan and Kendeng Thrust Fault
572 north of Madiun, East Java, Indonesia.

573

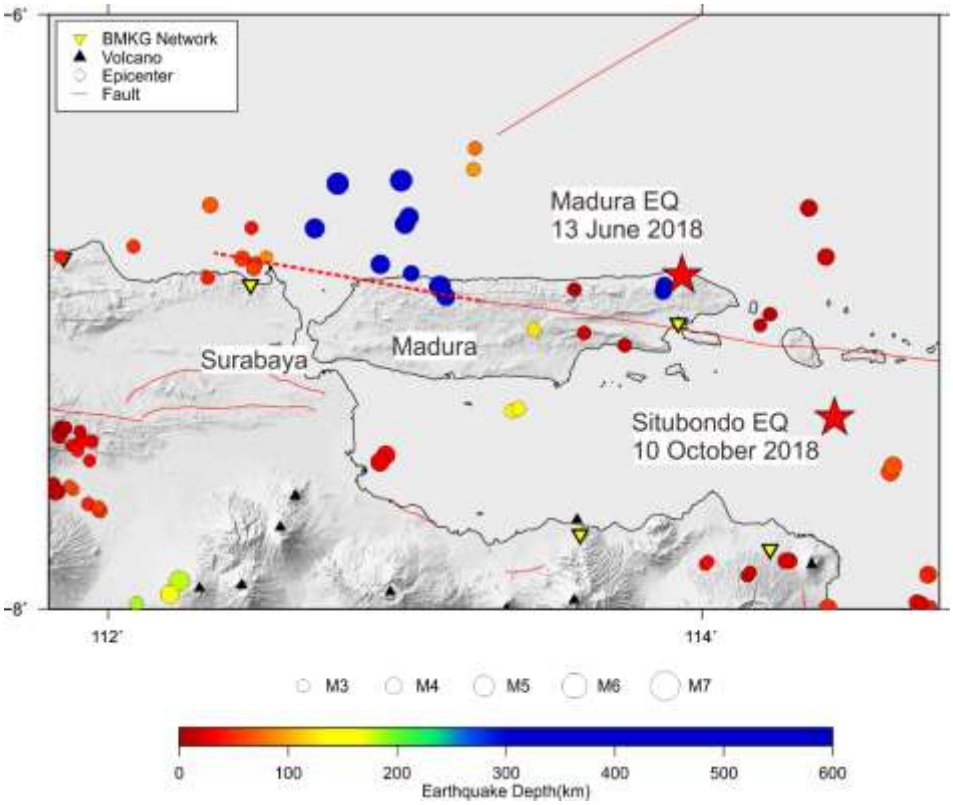

Fig. 11. Map of seismicity distribution around Rembang and Madura areas. The dashed red line is a possible extended fault). Red stars are recently earthquake occurred in 2018.

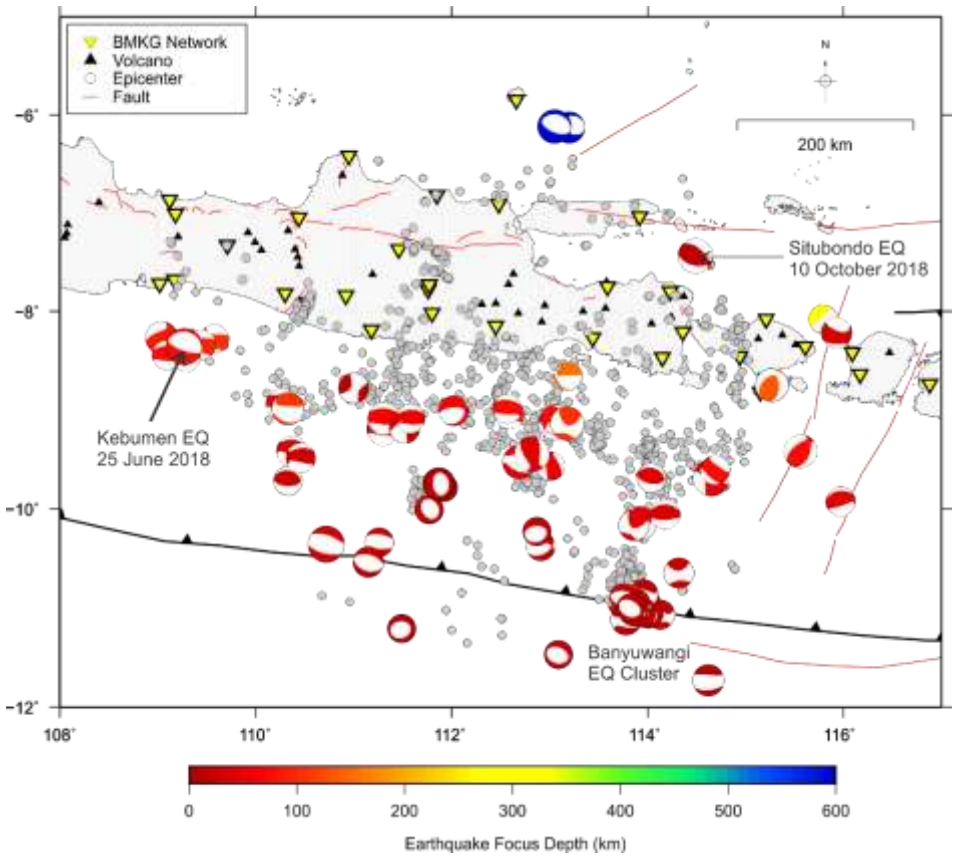

Fig. 12. Map of focal mechanism distribution around Central and East Java, taken from Global Centroid Moment Tensor (GCMT) (Dziewonski et al. 1981; Ekström et al. 2012) (https://www.globalcmt.org/) in the times period of 2009-2018. Grey dots are relocated epicentre.

Additional file(s):

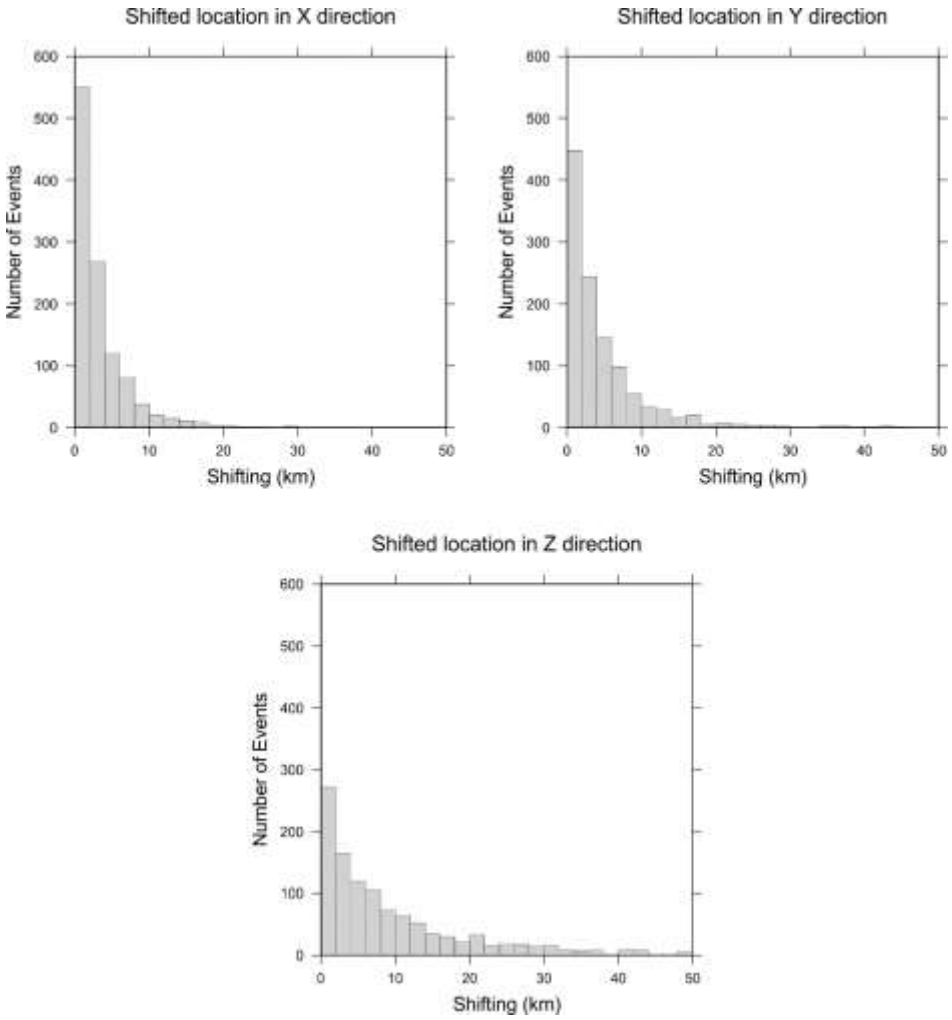

Fig. A1. Histograms of shifted earthquake locations in X, Y, and Z direction after relocation process by using double-difference algorithm with waveform cross-correlation.

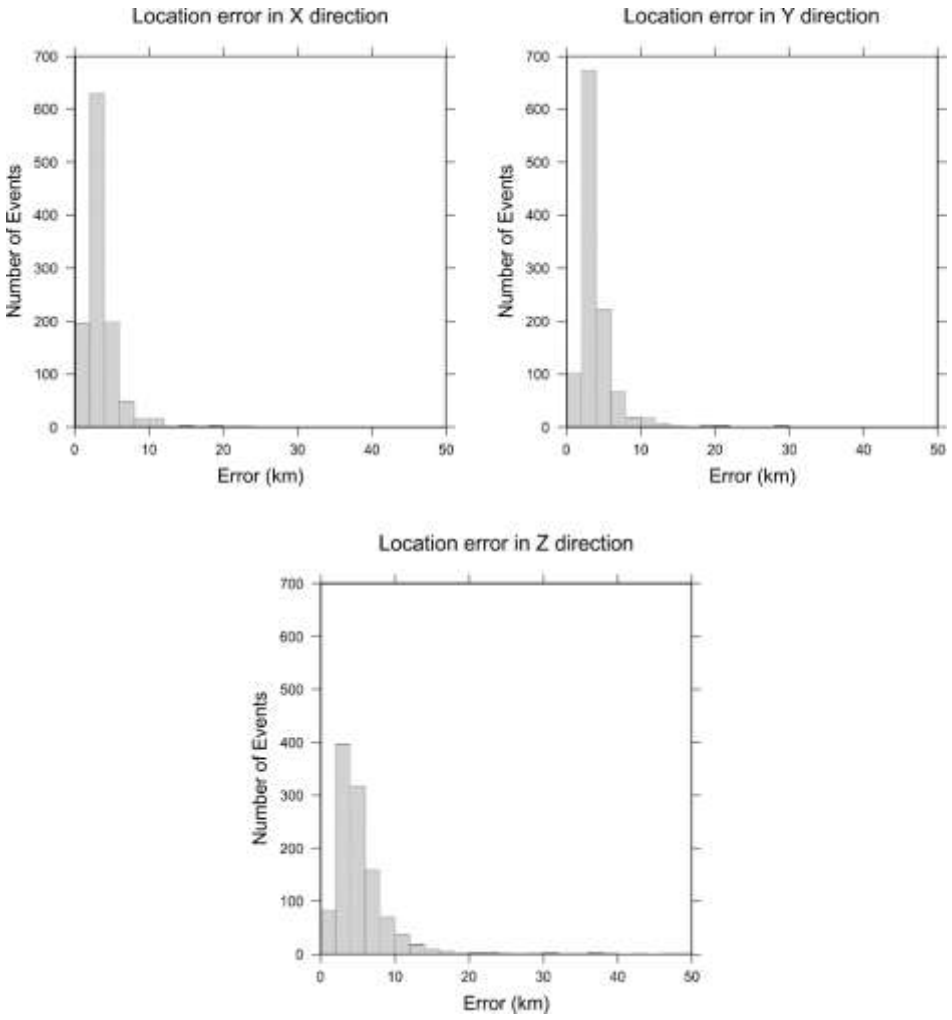

Fig. A2. Histograms of earthquake locations error in X, Y, and Z direction after relocation process by using double-difference algorithm with waveform cross-correlation.